Environmental Science & Technology

pubs.acs.org/est

Policy Analysis

When Bigger Is Not Greener: Ensuring the Sustainability of Power-to-Gas Hydrogen on a National Scale

Boris Brigljević, Manhee Byun, Hyunjun Lee, Ayeon Kim, Boreum Lee, Changhwan Moon, Jae Hyung Choi, Hyung Chul Yoon, Chang Won Yoon, Yong Sik Ok,* Dong-Ha Lim,* Chang-Hee Kim,* Sangbong Moon,* and Hankwon Lim*

Cite This: *Environ. Sci. Technol.* 2022, 56, 12828−12837

Read Online

ACCESS | Metrics & More | Article Recommendations | Supporting Information

ABSTRACT: As the prices of photovoltaics and wind turbines continue to decrease, more renewable electricity-generating capacity is installed globally. While this is considered an integral part of a sustainable energy future by many nations, it also poses a significant strain on current electricity grids due to the inherent output variability of renewable electricity. This work addresses the challenge of renewable electricity surplus (RES) utilization with target-scaling of centralized power-to-gas (PtG) hydrogen production. Using the Republic of Korea as a case study, due to its ambitious plan of 2030 green hydrogen production capacity of 0.97 million tons year^{-1}, we combine predictions of future, season-averaged RES with a detailed conceptual process simulation for green H_2 production via polymer electrolyte membrane (PEM) electrolysis combined with a desalination plant in six distinct scale cases (0.5−8.5 GW). It is demonstrated that at scales of 0.5 to 1.75 GW the RES is optimally utilized, and PtG hydrogen can therefore outperform conventional hydrogen production both environmentally (650−2210 Mton CO_2 not emitted per year) and economically (16−30% levelized cost reduction). Beyond these scales, the PtG benefits sharply drop, and thus it is answered how much of the planned green hydrogen target can realistically be "green" if produced domestically on an industrial scale.

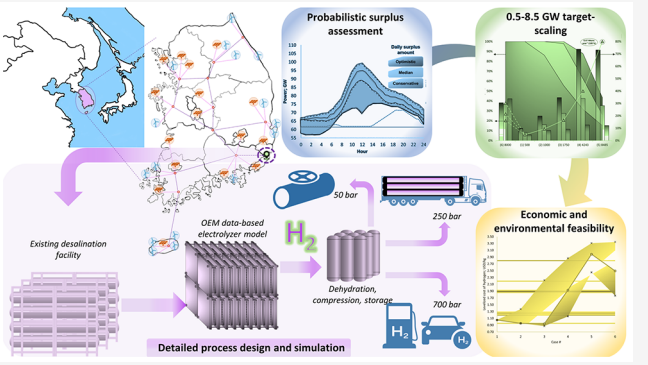

KEYWORDS: *renewable electricity surplus, target scaling, power-to-gas, PEM electrolysis, green H_2*

1. INTRODUCTION

Global awareness of climate change as a result of fossil-based energy consumption is constantly increasing.[1,2] Hence nation-wide strategies are implemented for a meaningful increase in renewable energy generation capacity,[3−6] particularly focusing on wind turbine and photovoltaic capacity as they are the most established technologies from an end-consumer basis.[7] Even though the goals of these strategies (increased energy security and environmental sustainability) are of the utmost importance for any nation, they also produce significant strains on electricity grid management. This is primarily due to the daily and seasonal fluctuation of renewable electricity availability (i.e., night−day cycle, wind intermittency, cloud coverage, etc.). Vast amounts of renewable electricity surplus (RES) can be generated at times when renewable electricity supply is abundant, but the demand for electricity is low, which can lead to inefficient usage of grid infrastructure or waste energy. This, in turn, necessitates RES storage and utilization strategies as they reduce the pressure on the electrical grid and store the energy which would otherwise have been wasted.[8−14] Among numerous energy storage concepts utilized such as batteries, compressed air, recirculating hydro, and super-conducting magnetic,[15,16] hydrogen (H_2) takes the spotlight due to its high energy density (120 MJ/kg), coupled with a potential for low to zero carbon emission in power-to-gas (PtG) systems assuming renewable electricity availability.[17] Besides energy storage, hydrogen is widely utilized as a raw material by major industries such as chemical, petrochemical, and metallurgical, whereas future utilization will also include transportation and stationary power generation enabled by fuel cell technology. Consequently, a plethora of research on renewable electricity-powered PtG systems has been conducted.

Detz et al. (2018)[18] performed a techno-economical assessment (TEA) of various fuels using renewable electricity where representative water electrolysis systems were inves-

Received: January 12, 2022
Revised: August 4, 2022
Accepted: August 5, 2022
Published: August 29, 2022

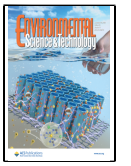

https://doi.org/10.1021/acs.est.1c08525
Environ. Sci. Technol. 2022, 56, 12828−12837

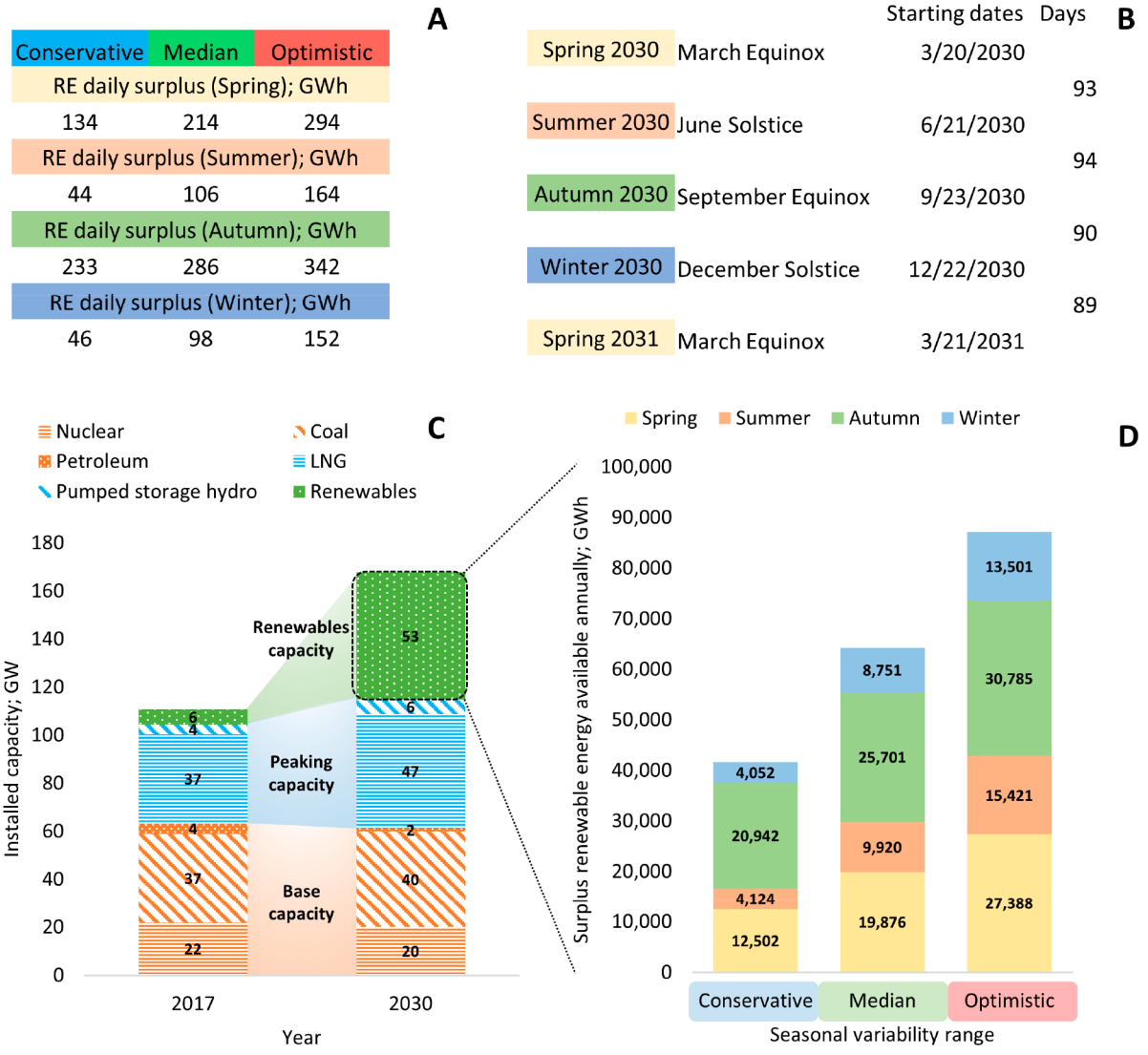

Figure 1. (A) Daily RES estimates on an averaged seasonal day. (B) Number of days of the seasons in 2030. (C) Electrical energy generation breakdown and total capacity values for the Republic of Korea in 2017 and predicted values for 2030.[30] (D) Conservative, median, and optimistic RES annual availability and seasonal distribution.

tigated as an H_2 source. Solid oxide electrolysis was confirmed to be economically competitive at a levelized cost of H_2 of 1.4 \$ kg^{-1} assuming technical improvements through learning rate by 2027. Glenk and Reichelstein (2019)[19] conducted a comprehensive profitability analysis for H_2 production from wind energy, reporting H_2 production costs of 3.41 \$/kg H_2 and 3.53 \$/kg H_2 for Germany and the USA, respectively. Koumi Ngoh and Njomo (2012)[20] compared three types of H_2 production using solar power with techno-economical aspect. The hydrogen production cost of 3.49 \$/kg H_2 in a larger production scale than 4000 tons $year^{-1}$ compared to thermal power-plant-based electricity was reported. Parra et al. (2017)[21] reported 85.6 \$ MWh^{-1} as the most competitive hydrogen production cost at 1 GW electrolyzer capacity and assuming heat and oxygen sold as byproducts. Decker et al. (2019)[22] conducted location analysis for an off-grid power-to-fuel system assuming 8000 h operation and reported optimal costs for electricity and H_2 of 40.08 \$ MWh^{-1} and 3.45 \$/kg H_2 in Germany. Abdin et al. (2019)[23] identified a minimum hydrogen production cost of 20.0 \$/kg H_2 and minimum costs of energy of 0.61 \$ kWh^{-1} for an integrated photovoltaic, wind turbine, and battery tank in the USA. Nadaleti et al. (2019)[24] predicted potential H_2 production using surplus energy in Brazil and reported H_2 production rates of 6.5−20 billion m^3 $year^{-1}$ with 1−3 h/day surplus energy available. Tlili et al. (2019)[25] suggested that interconnection between surplus energy and current H_2 production from nuclear energy can increase the availability of renewable electricity surplus by 82% and increase H_2 production capacity by a factor of 20. Maggio et al. (2019)[26] summarized the framework for H_2 production via electrolysis as (1) electricity generation from surplus energy in the order of tens of TWh, (2) long-term investment (10−20 years), and (3) elimination/reduction of taxation. Brey (2020)[27] reported that only 7.27 TWh surplus renewable electricity can be utilized to produce H_2 using existing natural gas infrastructure in Spain and quantified CO_2 emission reduction in 2030. Jacobson et al. (2017)[28] developed an energy roadmap where all energy sectors of 139 countries are replaced by wind, water, and sunlight (WWS) by 80% in 2030 and by 100% in 2050 total power demand (12.11 TW). It was outlined that by implementing 100% WWS by 2050 various financial benefits can be achieved by avoiding health costs of

https://doi.org/10.1021/acs.est.1c08525
Environ. Sci. Technol. 2022, 56, 12828−12837

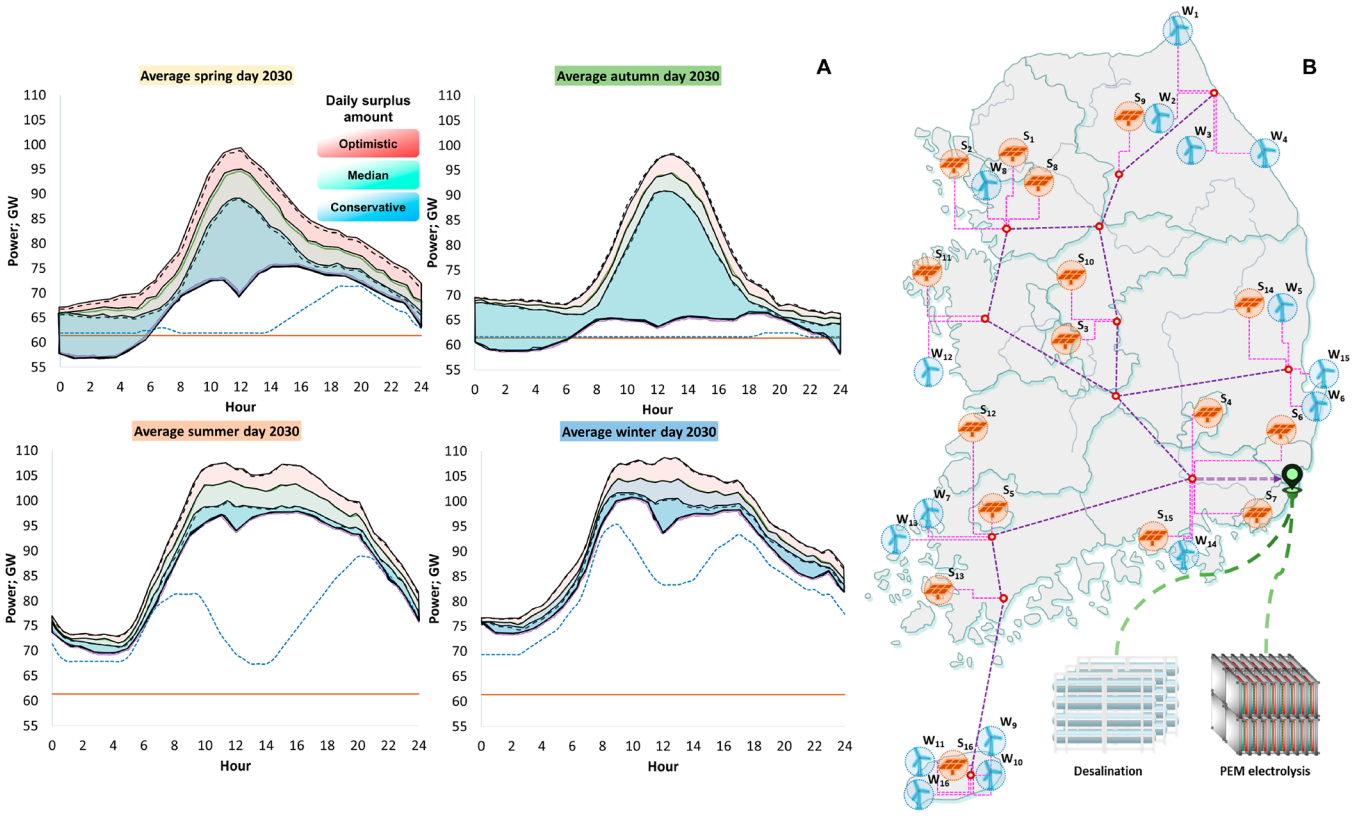

Figure 2. (A) Results of average seasonal day estimations of 2030 renewable electricity surpluses. Detailed explanation of the estimation is outlined in the Supporting Information extended methods section and Figure S9. (B) ROK's installed renewable capacities in 2030, consisting of wind parks (blue symbols), and solar parks (orange symbols) with corresponding capacities and geo-coordinates outlined in Table S8.

air pollution ~23 T$ year^{-1}, global-warming cost of ~28.5 T$ year^{-1}, which translated into 5800 $ year^{-1}/person. The same group (2019)[29] also focused on grid stability of 143 countries, where >99.7% of global fossil-fuel-based CO_2 emissions occur, with 80−100% energy transition of 20.26 TW in 2030−2050. Here, reductions for end-use energy of 57%, the private energy cost of 61%, and social cost of 91%, and the number of created full-time jobs of 28.6 million were reported.

Table S10 summarizes CAPEX, efficiency, capacity factors, electricity price, and cost of H_2 from the referenced works in the introduction.

In this work, we combine estimations of future (2030) nationwide renewable electricity surpluses as well as their daily and seasonal variations with a power-to-gas (PtG) hydrogen production on a scale that ensures competitive economics and maximized surplus utilization. Results of this work have broad and applicable implications as they (1) quantify the price of produced hydrogen (levelized cost and minimum selling price) and carbon emissions (per kg H_2) in a wide production scale range, (2) are subjected to various degrees of renewable electricity variability, and (3) are objectively compared with conventional hydrogen production through steam methane reforming (SMR) including and excluding carbon capture and sequestration (CCS).

2. METHODS

The essential methodology included in the main text consists of the renewable energy surplus assessment for 2030 and a detailed description of the process design. A more comprehensive methodology section including an explanation of the RES assessment assumptions, a description of Republic of Korea (ROK) as a case study, electrolyzer technology selection, economic analysis methods, and CO_2 emission calculations can be found in the Supporting Information.

2.1. Renewable Electricity Surplus Assessment. The Republic of Korea is a particularly interesting case study for this type of analysis primarily due to objectively ambitious goals for the installed renewable electricity (wind and solar) capacity in 2030 (Figure 1C). The root causes of which are predominately rising environmental as well as geopolitical (energy security) concerns combined with a significantly developed economy and technological know-how. The relatively high ratio of the planned wind and solar capacity to total generating capacity (~32%) dictates serious considerations for the management of the expected renewable electricity surpluses (RES) for both seamless operation of the energy grid as well as for ensuring the planned goals for hydrogen (green and conventional) in the upcoming decades. The numerical values of surface areas (in GWh) from Figure S9C,F,I,L are outlined in Figure 1A, while the duration of each season in 2030 is presented in Figure 1B. Figure 1D contains the product of values from Figure 1A,B, where the daily surplus estimation of a season is multiplied by the number of days in that season. Hence, as a result, we get conservative (41.6 TWh), median (64.2 TWh), and optimistic (87.1 TWh) annual renewable electricity surplus estimates as well as their seasonal variations. The assessment of the expected annual amount of RES as well as the seasonal variability (Figure 1D) inherent to wind turbines and solar photovoltaics was performed utilizing the data from a comprehensive 2018 report of the Korean Energy Economics Institute.[30]

https://doi.org/10.1021/acs.est.1c08525
Environ. Sci. Technol. 2022, 56, 12828−12837

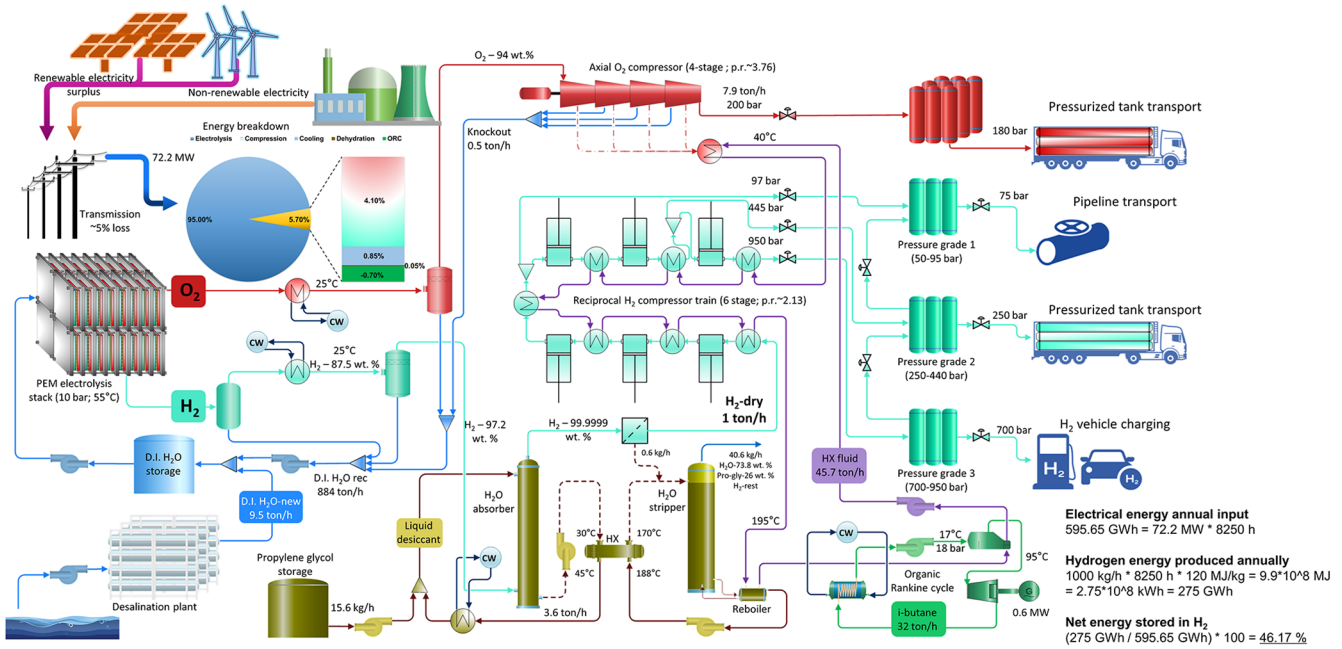

Figure 3. Main process design (process flow diagram) for a representative scale of 1 ton/h of hydrogen production.

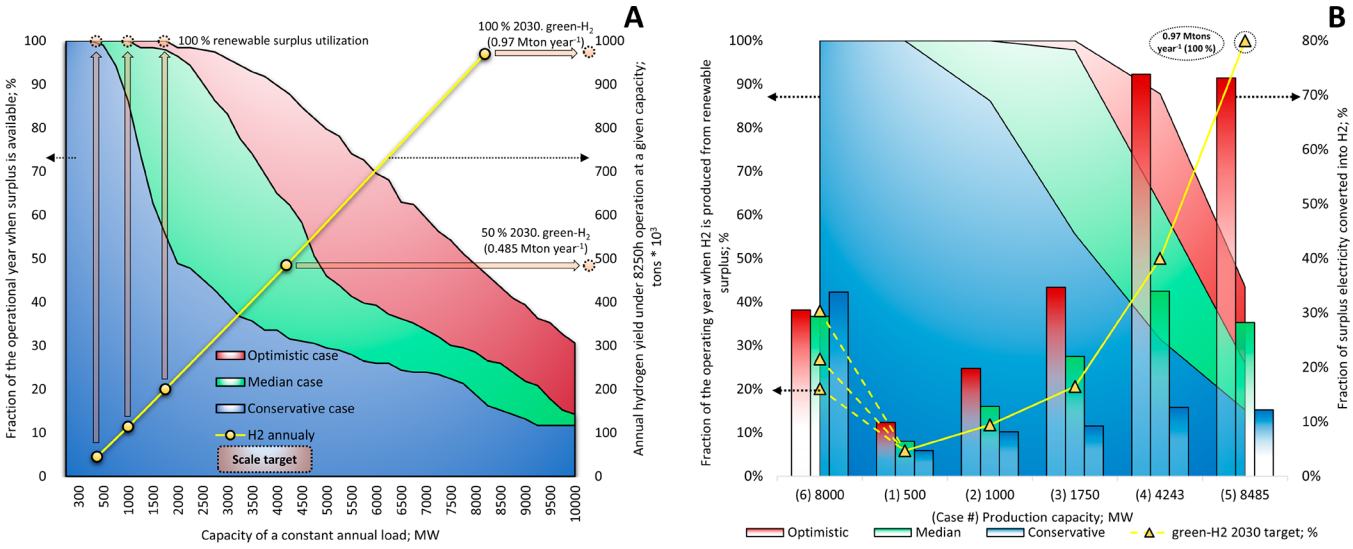

Figure 4. (A) Scope of the analysis with five distinct H_2 production capacities ranging from 500 to 8500 MW. The orange arrows and markers illustrate set targets for each of the cases. (B) Cases 5 and 6 (seasonal) production showing the relationship of production capacity (*x*-axis), % of year when H_2 is produced from RE surplus (left *y*-axis; surface plots), annual H_2 yield (left *y*-axis; yellow line and markers; % of 2030 green H_2 target), and amount of RE surplus utilized (right vertical axis; bar plots).

The main data that were utilized consisted of geographical locations and future capacities of wind and solar parks in SK (Figure 2B and Table S8), nonrenewable electricity generation capacity and breakdown, daily electricity demand curves (averaged to a typical seasonal day) and combined solar and wind electricity generation (based on localized weather patterns) including daily and seasonal variability. The processed data was used to produce daily assessments of electrical availability (demand and supply breakdown) in SK on four average seasonal days which was the basis for determining the amounts of RES in three distinct subcases (conservative, median, and optimistic) Figure 2A. These average seasonal day charts were generated with certain assumptions regarding stable grid operation in 2030 which consisted of (1) constant base generation capacity, (2) peaking generation capacity gradient is optimized to correspond to variable renewable electricity output, and (3) grid operators consider a conservative estimate of renewable electricity output on a given average seasonal day as a safety margin. The RES hourly profiles presented as absolute values are outlined in supplementary Figures S1−S3.

On an annual basis, it was determined that the total amount of RES in 2030 could range from 41.6 to 87.14 TWh with a median value of 64.2 TWh (Figure 3B), which is a direct cumulative effect of the daily RES availability ranges (Figure 4A). Furthermore, each annual value of the RES can be seen as a sum of different RES seasonal availabilities, and in this particular case of SK, the highest amounts of RES are

https://doi.org/10.1021/acs.est.1c08525
Environ. Sci. Technol. 2022, 56, 12828−12837

generated during autumn and spring (50−35 and 30−31% of the total annual RES, respectively). This, in turn, required careful consideration of a feasible (technologically reliable) PtG technology type (Supplementary Information; Extended methods; section 2) and perhaps, more importantly, the scale of the process.

2.2. PEM-WE Hydrogen Production and Processing Design. The conceptual process design strived to realistically encompass all the necessary operations for a stable output of pure and consumer-ready (pressurized) hydrogen. The scope of the process (Figure 3) encompasses the primary energy input (renewable electricity surplus and nonrenewable electricity), how that energy is utilized (energy breakdown), PEM water electrolysis (steady-state model follows the operational data provided by Elchemtech LLC), water desalination plant output (main feedstock supply, blue line), hydrogen (light green line) and oxygen (red line) downstream processing (water removal, compression with intercooling) and storage. Hydrogen dehydration (removal of trace amounts of water) is achieved using a liquid−liquid dehydration column with recirculating, nontoxic liquid desiccant (brown line). Both compressor stations are cooled with a heat exchange liquid (purple line) which transfers the heat to the H_2O stripper reboiler and the organic Rankine cycle which utilizes isobutane (dark green line) as the working fluid.

The process starts with pure demineralized water as the main feedstock (product of the desalination plant) which is pumped to a working pressure of the PEM electrolyzer. Even though this system can operate at considerably higher pressures (up to 350 bar) 10 bar was chosen due to case-specific governmental safety restrictions. Other operating parameters such as cell current density, water conversion, and temperature were obtained from an industrial collaborator (Elchemtech Ltd.) which manufactures and operates large-scale PEM electrolyzer systems. In terms of energy balance, 95% of the electrical energy requirement is reserved for the electrolysis stack while the majority of the remaining 5% is utilized for gas compression.

H_2 and O_2 exit the electrolysis stack in a vapor−liquid stream with the unconverted water at 50−60 °C. They are both cooled to room temperature, and the bulk of the water is recirculated to the electrolyzer. O_2 is compressed in a cooled axial compressor to a storage pressure of 180−200 bar, where the remaining water is removed as a knockout liquid from the compressor, and at this point, O_2 is considered a valuable product. Hydrogen on the other hand required a bit more challenging water removal and compression operations. As it exits the electrolysis stack, the water is first separated at the exit temperature, followed by a separation after cooling at room temperature. These two separations result in a hydrogen stream of ∼97.2 wt % purity. As this is an unacceptable level of purity for the final product the extra water content is removed by contacting it with a liquid (nontoxic) desiccant in an absorber tower. The column's top stream is filtered for the trace amounts of the desiccant and the resulting vapor is pure dry hydrogen. Liquid desiccant water removal was chosen instead of the somewhat more popular in-line solid bed adsorption (Si-based) because it allows fully continuous operation with optimized recycling (H_2O stripper) which becomes economically advantageous at large production scales which is considered in this study. Dry hydrogen is then compressed to three different pressure grades using a 6-stage reciprocal compressor train with intercooling. Parts of the hydrogen are taken out after the third, fifth, and final compression stage at pressures of 97, 445, and 950 bar, respectively. This, in turn, allows for intermediate storage which provides a steady supply for different grades of utilization consisting of pipeline transport (∼50 bar), pressurized tank transport (∼250 bar), and fuel cell vehicle charging (700 bar).

Consistent compressor cooling duty (both for O_2 and H_2 compression) is achieved with a heat transfer fluid (Dowtherm Q[31]), which is then used to provide a heating duty for the H_2O stripper column reboiler. As it exits the reboiler, the heat transfer liquid is cooled back to 40 °C by giving off heat in the boiler of the organic Rankine cycle (ORC). The working fluid in the ORC is isobutane at 18 bar and 95 °C before expansion.[32] The ORC was introduced as the last heat sink for the heat transfer fluid as well as another safety feature of the entire hydrogen production system since in the unlikely case of grid power failure the ORC would utilize the work from turbine inertia to purge the hydrogen from the system, and transfer water and glycol desiccant to storage tanks.

3. RESULTS AND DISCUSSION

3.1. Target-Scaling of PtG for Renewable Electricity Surplus Storage. The scope of the analysis was defined by combining the estimated data of annual RES availability with various scale cases (5 + 1) of the proposed hydrogen production process design ranging from 500 MW to 8500 MW. Figure 4A shows PEM electrolysis scale cases of 500, 1000, 1750, 4243, and 8485 MW (cases 1−5, respectively). This corresponds to annual hydrogen production of 0.057, 0.114, 0.200, 0.485, and 0.970 Mton. Each of the cases from 1 to 5 had an assumed constant annual operation of 8250 h, whereas case 6 was introduced to illustrate the effects of a large-scale operation in RES peak times only (outlined in the last paragraph of the section). In the operational year, the renewable electricity surplus availability will be varying as it was shown in Figure 1D. Scales of cases 1−3 (500, 1000, and 1750 MW) were targeted (or maximized) so that the process operates from a renewable electricity surplus of 100% of the operational time in conservative, median, and optimistic estimates. In other words, they operate 100% of the operational time from renewable electricity surplus (RES), which ensures that all of the produced H_2 is without indirect carbon emissions. Therefore, in a conservative estimate, a PEM electrolysis system of 500 MW capacity can operate for 8250 h, 100% from renewable electricity surplus. Likewise, the 1000 and 1750 MW systems can also operate 100% of the time from renewable electricity surplus in a median and optimistic estimate, respectively.

In terms of annual hydrogen output, these scales correspond to 0.057, 0.114, and 0.2 Mton. Given that the green H_2 target for the ROK in 2030 is 0.97 Mton, cases 1−3 (500, 1000, and 1750 MW), correspond to 6, 12, and 21% of the green H_2 target.

Cases 4 and 5 were scaled for 50 and 100% of the ROK green hydrogen target for 2030 (0.97 Mton). In those cases (due to their scales), they did not operate 100% of the time from renewable electricity surplus. Case 4 operated from a renewable electricity surplus of 31.5, 62.4, and 87.8% of the time in conservative, median, and optimistic estimates, respectively. Likewise, case 5 operated from a renewable electricity surplus of 15.2, 25.9, and 43.5% of the time in conservative, median and optimistic estimates, respectively.

https://doi.org/10.1021/acs.est.1c08525
Environ. Sci. Technol. 2022, 56, 12828−12837

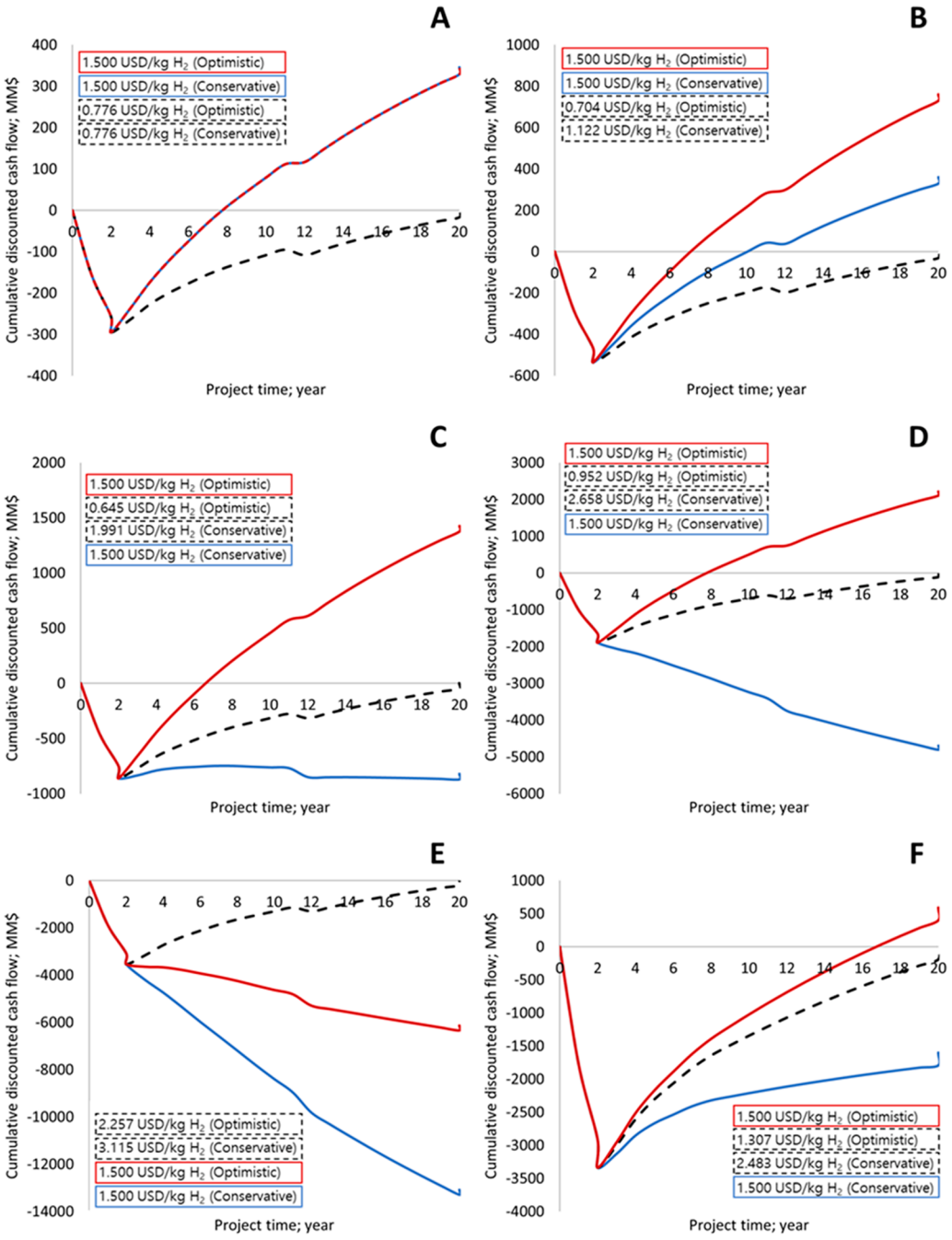

Figure 5. Profitability analyses for 20 years of project life for cases 1−6 (A−F, respectively). Red (optimistic) and blue (conservative) curves for cumulative cash flow (CCF) with H_2 price of 1.5 USD kg^{-1}. Dashed curves CCFs at minimum hydrogen selling prices (legend values).

The implications of these production scales in relation to annual RES availability are made clear in Figure 4B where it was quantified how much of the RES can be utilized, while simultaneously showing the amount of the operational year where the process actually operates from RES and when it operates from other electricity sources. On the right *y*-axis of Figure 4B, it can be seen how much of the total surplus electricity available annually is converted to H_2 at each PEM electrolysis scale. Hence, cases 1−5 can convert 5−12% (blue bars), 6−34% (green bars), and 10−74% (red bars) in conservative, median, and optimistic estimates of RES annual availability. Yellow lines and markings signify the annual hydrogen output as a percentage of 2030 ROK's green hydrogen target, hence with increasing PEM electrolysis scale from case 1 to case 5 these values increase from 6 to 100%. However, as can be seen on the left *y*-axis of Figure 4B, as the scale increases from case 1 to case 5, the amount of operating time when hydrogen is produced from RES decreases. This implies that (assuming constant operation throughout the year) hydrogen can be produced without indirect CO_2 emissions at 500 MW PEM capacity (case 1) considering conservative RES availability estimation and at 1750 MW PEM capacity (case 3) considering optimistic RES availability estimation. At higher scales in cases 4 and 5, if median RES availability estimation is considered, they operate from RES 62 and 32% of the operational year. This, of course, implies that for the rest of the operational year those cases do not produce emission-free (green) hydrogen.

https://doi.org/10.1021/acs.est.1c08525
Environ. Sci. Technol. 2022, 56, 12828−12837

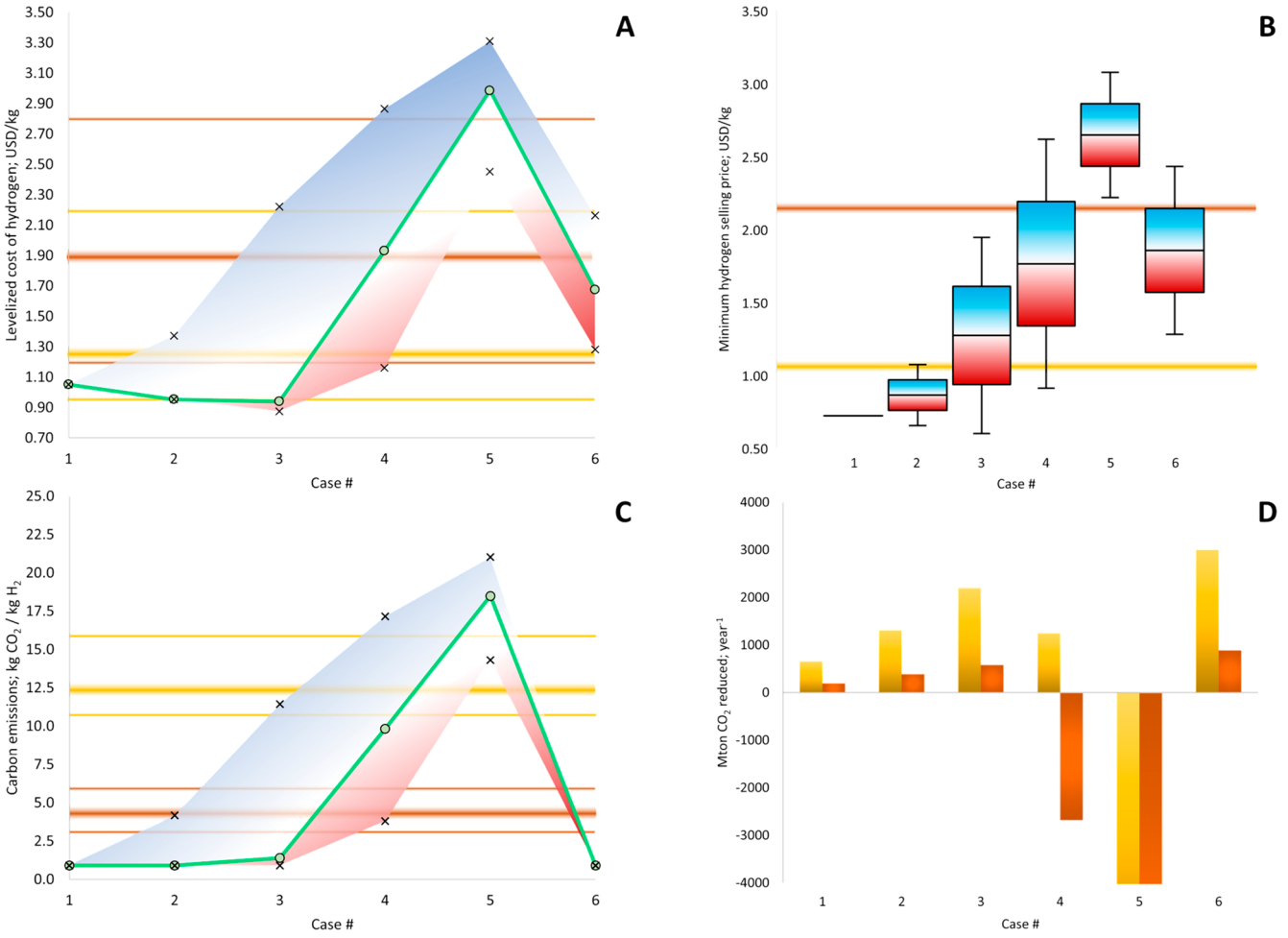

Figure 6. Median (green line), conservative (blue surface), and optimistic (red surface) levelized cost of hydrogen (LCOH). Thick and thin lines are the median and mix/max LCOH from steam methane reforming (SMR; yellow) and steam methane reforming with carbon capture and sequestration (SMR + CCS; orange). (A) Minimum hydrogen selling price (MHSP) ranges (bar and whiskers plots). SMR MHSP (yellow); SMR + CCS MHSP (orange). (B) Median (green), optimistic (red surface), and conservative (blue surface) CO_2 emissions. Yellow and orange lines; SMR, SMR + CCS CO_2 emissions. (C,D) Median annual CO_2 emission reduction compared to equal H_2 production scale from SMR (yellow) and SMR+CCS (orange).

The analysis is also widened by an additional case (6) where the production scale is relatively large (8000 MW), but the operation is seasonal to match the RES seasonal peaks in spring and autumn (Figures S1−S3). A capacity of 8000 MW was chosen since it was determined that maximum RES can be utilized at the constant operation during spring and summer (Figure S4). Considering median, optimistic, and conservative RES availability in autumn and spring, it can be seen how in case 6 daily operational time is tuned accordingly in Figures S5 and S6, respectively. Due to its seasonal operation case 6 produces significantly less H_2 annually (when compared to the similarly sized system in case 5) and can satisfy 20−38% of 2030 green hydrogen target (Figure 4B; case 6; yellow markings). However, all of the H_2 produced is 100% from RES which makes case 6 the middle ground between large annual H_2 output (cases 4 and 5) and environmental sustainability (cases 1, 2, and 3).

3.2. Economic and Environmental Implications Compared to Conventional Hydrogen Production. From the discounted cash flow diagrams (DCFDs) in Figure 5 (detailed results available in Tables S5 and S6), the net present value (NPV), the minimum H_2 selling price (MHSP), the discounted payback period (DPBP), and the discounted cash flow rate of return (DCFROR) were identified for each case. For instance, 360.5 and 760 million USD of NPV can be observed in Case 2 (Figure S8B) utilizing MHSP and commercial H_2 selling price of 1.5 USD/kg for conservative and optimistic scenarios, respectively. The positive and negative NPVs represent profitable and unprofitable cases, respectively. Discounted payback period (DPBP, Table S5) is the required time to retrieve the investment for the project. DCFROR (Table S5) is the discounted rate when the NPV value is zero at the end of the lifespan of the project. Minimum H_2 selling price (MHSP) is the calculated H_2 selling price when the NPV value is zero at the end of the lifespan of the project, or in other words the guarantee that there is no financial deficit. From these results, it can be clearly shown that higher power capacity, higher operating time, and relatively higher RSSA use, result in the CAPEX reduction due to the economy of scale, the low H_2 production cost owing to the higher H_2 production rates, and lower annual electricity price, respectively, were necessary to obtain higher profit (Figure 5D, optimistic). Furthermore, it is also clear that the profitability of the project has a direct causal relationship with the amount of time the process operates from RES which can be seen in both conservative and optimistic scenarios of Figure 5 where, as you

https://doi.org/10.1021/acs.est.1c08525
Environ. Sci. Technol. 2022, 56, 12828−12837

go up in production scale (from case 1 to case 5) the less likely it is that the process will operate from RES. Furthermore, it can be observed that in conservative estimate of RES availability the process stops being profitable after case 2 (Figure 5B) or 1 GW capacity with 86.2% of annual RES available (assuming constant operation). Similarly, in an optimistic estimate the last profitable case 4 (Figure 5D) utilizes 87.8% of RES at 4.3 GW capacity. This entails that scaling the process between 1 and 4.3 GW will likely result in profitable economic performance, with maximum utilization of RES throughout the entire operational year. In case 6, the capacity is maximized (8 GW) for optimal utilization of RES seasonal peaks in autumn and spring (Figures S4−S6). As it operates seasonally, the annual output is comparable to that of case 3 (1.75 GW), but the hydrogen produced is more sustainable due to maximum RES utilization. Economically, this translates into a profitable scenario but over longer project lifetime (Figure 5F) if we consider the conservative RES scenario.

The final results of this analysis pertain to cost estimations, profitability assessment, as well as CO_2 emissions for each case and comparison to conventional hydrogen production routes from steam methane reforming (SMR) and steam methane reforming including carbon capture and sequestration (SMR + CCS) (Figure 6). The results of each comparison criteria are presented as a range of values from the most optimistic (red) to the most conservative extreme (blue) which is a direct consequence of RES annual availability variation. Yellow and orange horizontal lines represent the comparison values (as well as ranges in Figure 6A,C) for SMR and SMR + CCS respectively. As can be observed, cases 1 and 2 have the highest degree of certainty (even considering the most conservative case scenario) of economically outperforming conventional SMR and SMR + CCS (Figure 6A,B), whereas cases 3, 4, and 6 more likely stand to outperform only SMR + CCS. On the other hand, cases 1, 2, 3, and 6 all stand to outperform SMR + CCS and SMR environmentally (Figure 6C), which clearly indicates the nationwide potential of CO_2 emissions reduction. Specifically, if the same amount of H_2 was switched from SMR to PtG in scales from cases 1, 2, 3, and 6, this would result in annual CO_2 emission reductions of 660, 1315, 2200, and 3005 million tons, respectively (Figure 6D).

3.3. Result Implications. By combining nationwide planned electricity generation capacity, seasonal renewable electricity surplus (RES) availability estimations, and variation ranges with rigorous process design and techno-economic and environmental assessment, this study has quantitatively demonstrated the optimal scales of electrolytically produced hydrogen in terms of minimized carbon emissions and maximized production capacity. The analysis was performed with the Republic of Korea as a case study for 2030 using a centralized green hydrogen production process from PEM electrolysis combined with an existing desalination plant. With an annual estimated RES range of 41.6 to 87.14 TWh, we have determined that a hydrogen production of 57−200000 tons/year is achievable utilizing RES. More specifically, the PEM electrolyzer of capacities ranging from 0.5 to 1.75 GW operating 8250 h/year can do so exclusively from RES. Furthermore, when operating in this scale range it was proven that the produced hydrogen will almost certainly outperform conventional steam methane reforming (SMR) routes both environmentally as well as economically. Interestingly, increasing the production scales to 50% and 100% (0.97 Mton/year) of the 2030 national target green H_2 capacity will not result in a better performance compared to SMR routes, due to less frequent utilization of the annual RES. In other words, even though PEM electrolysis powered by RES is a pathway for green hydrogen, there exists a maximum production scale where sustainability (or carbon emission-free production) can be guaranteed and above which the produced hydrogen cannot be considered entirely green. Large-scale, RES peak-targeted operation (case 6) might be the middle ground solution between these two extremes as it maximizes RES utilization and therefore ensures that the hydrogen produced is green, but it does so with the seasonal operation, making the produced hydrogen more expensive. As a final note, this case study unequivocally demonstrates that with strategic planning, PtG hydrogen on a national scale can indeed be environmentally and economically more feasible than conventional SMR routes provided that an optimal combination of the economy of scale regarding variable RES output is achieved. In that scenario, it can be utilized as both RES storage, and energy grid stabilization resource, thus providing a strong techno-economical argument for a realistic, hydrogen-powered future.

■ ASSOCIATED CONTENT

Supporting Information

The Supporting Information is available free of charge at https://pubs.acs.org/doi/10.1021/acs.est.1c08525.

Extended methodology section, absolute values of season-averaged, hourly RES values, details on the process simulation model, and economic assessment data (PDF)

■ AUTHOR INFORMATION

Corresponding Authors

Yong Sik Ok − *Korea Biochar Research Center, APRU Sustainable Waste Management Program and Division of Environmental Science and Ecological Engineering, Korea University, Seoul 02841, Republic of Korea;* orcid.org/0000-0003-3401-0912; Email: yongsikok@korea.ac.kr

Dong-Ha Lim − *Green Materials & Processes R&D Group, Korea Institute of Industrial Technology, Ulsan 44413, Republic of Korea;* orcid.org/0000-0003-4328-5168; Email: dongha4u@kitech.re.kr

Chang-Hee Kim − *Korea Institute of Energy Technology, Naju 58330, South Korea*; Email: chk14@kier.re.kr

Sangbong Moon − *Elchemtech Co. Ltd., Seoul 07795, Republic of Korea*; Email: sbmoon@elchemtech.com

Hankwon Lim − *School of Energy and Chemical Engineering and Department of Energy Engineering, Ulsan National Institute of Science and Technology, Ulsan 44919, Republic of Korea;* orcid.org/0000-0002-1074-0251; Email: hklim@unist.ac.kr

Authors

Boris Brigljević − *School of Energy and Chemical Engineering, Ulsan National Institute of Science and Technology, Ulsan 44919, Republic of Korea; Carbon Value Co., Ltd., Busan 48058, Republic of Korea*

Manhee Byun − *School of Energy and Chemical Engineering, Ulsan National Institute of Science and Technology, Ulsan 44919, Republic of Korea*

https://doi.org/10.1021/acs.est.1c08525
Environ. Sci. Technol. 2022, 56, 12828−12837

Hyunjun Lee − *School of Energy and Chemical Engineering, Ulsan National Institute of Science and Technology, Ulsan 44919, Republic of Korea*
Ayeon Kim − *School of Energy and Chemical Engineering, Ulsan National Institute of Science and Technology, Ulsan 44919, Republic of Korea*
Boreum Lee − *School of Energy and Chemical Engineering, Ulsan National Institute of Science and Technology, Ulsan 44919, Republic of Korea; Department of Chemical and Environmental Engineering, Yale University, New Haven, Connecticut 06520-8286, United States*
Changhwan Moon − *Elchemtech Co. Ltd., Seoul 07795, Republic of Korea*
Jae Hyung Choi − *Green Materials & Processes R&D Group, Korea Institute of Industrial Technology, Ulsan 44413, Republic of Korea*
Hyung Chul Yoon − *Clean Fuel Laboratory, Korea Institute of Energy Research, Daejeon 34129, Republic of Korea;* orcid.org/0000-0002-5607-7838
Chang Won Yoon − *Department of Chemical Engineering, Pohang University of Science and Technology (POSTECH), Pohang, Gyeongbuk 37673, Republic of Korea;* orcid.org/0000-0003-1221-6901

Complete contact information is available at: https://pubs.acs.org/10.1021/acs.est.1c08525

Notes

The authors declare no competing financial interest.

■ ACKNOWLEDGMENTS

This research was supported by the Hydrogen Energy Innovation Technology Development Program of the National Research Foundation of Korea (NRF) funded by the Korean government (Ministry of Science and ICT (MSIT)) (NRF-2019M3E6A1064290) and also supported by the Korea Institute of Energy Technology Evaluation and Planning (KETEP) granted financial resource from the Ministry of Trade, Industry & Energy, Republic of Korea (No. 20183010032380). This study has been conducted with the support of the Korea Institute of Industrial Technology as "Development of eco-friendly production system technology for total periodic resource cycle" (KITECH EO-21-0014). The first author would also like to acknowledge Mr. Jadranko Kučica, m.eng.e.e. the Head of Long-term Planning of Croatian Transmission System Operator Ltd. (HOPS) for professional advice in national electrical grid management strategies.

■ REFERENCES

(1) United Nations. *Adoption of the Paris Agreement; Fccc/Cp/2015/L.9/Rev.1*, 2015; p 32.
(2) United Nations. *Kyoto Protocol to the United Nations Framework Convention on Climate Change*, 1998; https://unfccc.int/resource/docs/convkp/kpeng.pdf (accessed 2022-08-12).
(3) Gielen, D.; Boshell, F.; Saygin, D.; Bazilian, M. D.; Wagner, N.; Gorini, R. The Role of Renewable Energy in the Global Energy Transformation. *Energy Strateg. Rev.* **2019**, *24*, 38−50.
(4) International Energy Agency. Germany 2020 Energy Policy Review; https://www.iea.org/reports/germany-2020 (accessed 2020-09-10).
(5) Korea Energy Agency. *Korea Renewable Energy 3020 Plan*, 2018; https://www.iea.org/policies/6569-korea-renewable-energy-3020-plan (accessed 2022-08-12).
(6) Department of Energy & Climate Change. *UK Renewable Energy Roadmap - Update 2013*; London, 2013.
(7) Zhao, P.; Xu, W.; Zhang, S.; Wang, J.; Dai, Y. Technical Feasibility Assessment of a Standalone Photovoltaic/Wind/Adiabatic Compressed Air Energy Storage Based Hybrid Energy Supply System for Rural Mobile Base Station. *Energy Convers. Manag.* **2020**, *206*, 112486.
(8) Chen, W.; Li, G.; Pei, A.; Li, Y.; Liao, L.; Wang, H.; Wan, J.; Liang, Z.; Chen, G.; Zhang, H.; Wang, J.; Cui, Y. A Manganese-Hydrogen Battery with Potential for Grid-Scale Energy Storage. *Nat. Energy* **2018**, *3* (5), 428−435.
(9) Young, J. L.; Steiner, M. A.; Döscher, H.; France, R. M.; Turner, J. A.; Deutsch, T. G. Direct Solar-to-Hydrogen Conversion via Inverted Metamorphic Multi-Junction Semiconductor Architectures. *Nat. Energy* **2017**, *2* (4), 1−8.
(10) Reuß, M.; Grube, T.; Robinius, M.; Preuster, P.; Wasserscheid, P.; Stolten, D. Seasonal Storage and Alternative Carriers: A Flexible Hydrogen Supply Chain Model. *Appl. Energy* **2017**, *200*, 290−302.
(11) Jiang, L.; Lu, Y.; Zhao, C.; Liu, L.; Zhang, J.; Zhang, Q.; Shen, X.; Zhao, J.; Yu, X.; Li, H.; Huang, X.; Chen, L.; Hu, Y. S. Building Aqueous K-Ion Batteries for Energy Storage. *Nat. Energy* **2019**, *4* (6), 495−503.
(12) Elliott, D. A Balancing Act for Renewables. *Nat. Energy* **2016**, *1* (1), 1−3.
(13) Mitchell, C. Momentum Is Increasing towards a Flexible Electricity System Based on Renewables. *Nat. Energy* **2016**, *1* (2), 15030.
(14) Drechsler, M.; Egerer, J.; Lange, M.; Masurowski, F.; Meyerhoff, J.; Oehlmann, M. Efficient and Equitable Spatial Allocation of Renewable Power Plants at the Country Scale. *Nat. Energy* **2017**, *2* (9), 1−9.
(15) Shatnawi, M.; Qaydi, N. Al; Aljaberi, N.; Aljaberi, M. Hydrogen-Based Energy Storage Systems: A Review. *7th Int. IEEE Conf. Renew. Energy Res. Appl. ICRERA 2018* **2018**, *2* (1), 697−700.
(16) Bonovas, M. I.; Anagnostopoulos, I. S. Modelling of Operation and Optimum Design of a Wave Power Take-off System with Energy Storage. *Renew. Energy* **2020**, *147*, 502−514.
(17) Blanco, H.; Faaij, A. A Review at the Role of Storage in Energy Systems with a Focus on Power to Gas and Long-Term Storage. *Renew. Sustain. Energy Rev.* **2018**, *81*, 1049−1086.
(18) Detz, R. J.; Reek, J. N. H.; Van Der Zwaan, B. C. C. The Future of Solar Fuels: When Could They Become Competitive? *Energy Environ. Sci.* **2018**, *11* (7), 1653−1669.
(19) Glenk, G.; Reichelstein, S. Economics of Converting Renewable Power to Hydrogen. *Nat. Energy* **2019**, *4* (3), 216−222.
(20) Koumi Ngoh, S.; Njomo, D. An Overview of Hydrogen Gas Production from Solar Energy. *Renew. Sustain. Energy Rev.* **2012**, *16* (9), 6782−6792.
(21) Parra, D.; Zhang, X.; Bauer, C.; Patel, M. K. An Integrated Techno-Economic and Life Cycle Environmental Assessment of Power-to-Gas Systems. *Appl. Energy* **2017**, *193*, 440−454.
(22) Decker, M.; Schorn, F.; Samsun, R. C.; Peters, R.; Stolten, D. Off-Grid Power-to-Fuel Systems for a Market Launch Scenario − A Techno-Economic Assessment. *Appl. Energy* **2019**, *250* (April), 1099−1109.
(23) Abdin, Z.; Mérida, W. Hybrid Energy Systems for Off-Grid Power Supply and Hydrogen Production Based on Renewable Energy: A Techno-Economic Analysis. *Energy Convers. Manag.* **2019**, *196* (June), 1068−1079.
(24) Nadaleti, W. C.; Borges dos Santos, G.; Lourenço, V. A. The Potential and Economic Viability of Hydrogen Production from the Use of Hydroelectric and Wind Farms Surplus Energy in Brazil: A National and Pioneering Analysis. *Int. J. Hydrogen Energy* **2020**, *45* (3), 1373−1384.
(25) Tlili, O.; Mansilla, C.; Robinius, M.; Syranidis, K.; Reuss, M.; Linssen, J.; André, J.; Perez, Y.; Stolten, D. Role of Electricity Interconnections and Impact of the Geographical Scale on the French Potential of Producing Hydrogen via Electricity Surplus by 2035. *Energy* **2019**, *172*, 977−990.
(26) Maggio, G.; Nicita, A.; Squadrito, G. How the Hydrogen Production from RES Could Change Energy and Fuel Markets: A

Review of Recent Literature. *Int. J. Hydrogen Energy* **2019**, *3*, 11371−11384.
(27) Brey, J. J. Use of Hydrogen as a Seasonal Energy Storage System to Manage Renewable Power Deployment in Spain by 2030. *Int. J. Hydrogen Energy* **2020**, *46* (33), 17447−17457.
(28) Jacobson, M. Z.; Delucchi, M. A.; Bauer, Z. A. F.; Goodman, S. C.; Chapman, W. E.; Cameron, M. A.; Bozonnat, C.; Chobadi, L.; Clonts, H. A.; Enevoldsen, P.; Erwin, J. R.; Fobi, S. N.; Goldstrom, O. K.; Hennessy, E. M.; Liu, J.; Lo, J.; Meyer, C. B.; Morris, S. B.; Moy, K. R.; O'Neill, P. L.; Petkov, I.; Redfern, S.; Schucker, R.; Sontag, M. A.; Wang, J.; Weiner, E.; Yachanin, A. S. 100% Clean and Renewable Wind, Water, and Sunlight All-Sector Energy Roadmaps for 139 Countries of the World. *Joule* **2017**, *1* (1), 108−121.
(29) Jacobson, M. Z.; Delucchi, M. A.; Cameron, M. A.; Coughlin, S. J.; Hay, C. A.; Manogaran, I. P.; Shu, Y.; von Krauland, A. K. Impacts of Green New Deal Energy Plans on Grid Stability, Costs, Jobs, Health, and Climate in 143 Countries. *One Earth* **2019**, *1* (4), 449−463.
(30) Cho, S.; Cho, I. Green Energy Research: Study of Grid Stability with the Increasing Penetration of Variable Renewable Energy. *Korea Energy Econ. Inst.* **2018**, *18*−*28* (7), 58.
(31) Dow Chemical Company. *DOWTHERM Q (Synthetic organic heat transfer fluid); Technical Data Sheet*; http://www.dowtherm.com (accessed 2020-09-25).
(32) Yang, A.; Su, Y.; Shen, W.; Chien, I. L.; Ren, J. Multi-Objective Optimization of Organic Rankine Cycle System for the Waste Heat Recovery in the Heat Pump Assisted Reactive Dividing Wall Column. *Energy Convers. Manag.* **2019**, *199*, 112041.

https://doi.org/10.1021/acs.est.1c08525
Environ. Sci. Technol. 2022, 56, 12828−12837